

Mechanosensitivity of fibroblast  
towards inertial shear force and  
microgrooved surface topography

WA Loesberg, XF Walboomers, JA Jansen, and JJWA van Loon

*Annals of Biomechanical Engineering, submitted, 2008*

## INTRODUCTION

The effects of fluid shear force on cell structure and function have been investigated in several studies. Especially, the effects of laminar flow and the associated wall shear stress on cells have been researched, since fluid shear is an important physiological phenomenon in blood vessels [1-4]. Besides endothelial cells, mechano-sensing and adaptation of bone is also often described to be governed by fluid shear forces [5-7]. A number of parameters have been measured: reorganisation of F-actin and intermediate filaments structures [8-12], extracellular matrix production (vinculin, fibronectin, integrin, collagen) [13; 14], the involvement of RhoA, the role of ion channels (Na<sup>+</sup>), and associated increases in ERK1/2 stimulation [15].

On a cellular level both fluid and inertial shear forces may use the same mechanotransduction pathways, whereby cells undergo changes in morphology as a response to mechanical signals. Inertial shear force can easily be generated under laboratory conditions in a fixed angle centrifuges. In standard centrifuges, either in regular laboratories or as control samples in space flight experiments, an essential difference between inertial shear force and gravity force is that inertial shear acts perpendicular to the gravity acceleration vector [16].

Force transmission from the extracellular matrix to the cell interior occurs through a chain of proteins, the focal adhesion sites, that are comprised of an integrin-extracellular matrix bond (e.g. vitronectin and fibronectin), integrin-associated proteins on the intracellular side (paxilin, tensin), and proteins linking the focal adhesion complex to the cytoskeleton (talin, vinculin). Stresses transmitted through adhesion receptors and distributed throughout the cell could cause conformational changes in individual force transmitting proteins, any of which would be a candidate for force transduction into a biochemical signal [17]. These integrin/focal adhesion mediated assemblies vice versa are dependant upon the activities of these signals, particularly the activity of the Rho family of GTPases. By subtly modulating pathways via soluble growth factors and differentiation factors, integrins also exerts their action through an indirect way. Antibody mediated engagement and clustering of integrins leads to activation of the Mitogen Activated Protein Kinase pathways, which are key effectors of these processes [18-20] (**Figure1**).

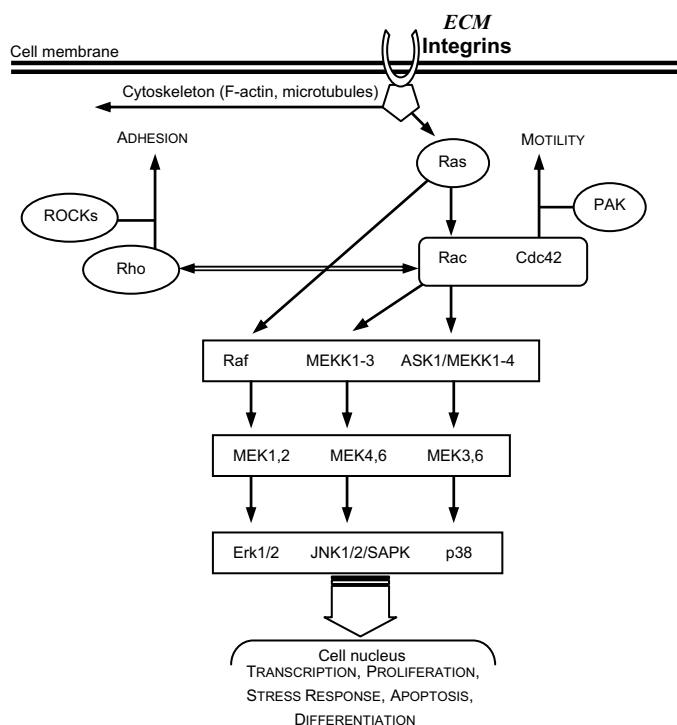


*Figure 1. Mitogen Activated Protein Kinases (MAPK) intracellular signalling pathways. A simplified schematic of the three major MAPK pathways and the members of the Rho family of small GTPases.*

Altered acceleration circumstances might have an effect on focal adhesion and actin polymerisation, both associated with integrins, which in turn control the signalling to MAPK. Although it has been shown that these kinases respond to a range of stimuli, little is known about the cellular response to changed shear conditions [21-23] [24-27]. In this study we applied a range of inertial shear forces on fibroblasts cultures on various micro-structured substrata. To ascertain the impact of inertial shear force we looked both at a morphological (scanning electron and fluorescence microscopy) and molecular level (mRNA transcription and Western blotting). The underlying aim was to understand to what extent inertial shear forces can alter directed cell behaviour, such as seen on microtextured substrates, and in addition, what parameter is more important in determining cell response.

## MATERIALS & METHODS

### *Substrata:*

Microgrooved patterns were made, using a photo lithographic technique and subsequent etching in a silicon wafer as described by Walboomers *et al.* [28]. The dimensions of the microgrooved topography were a ridge- and groove width of 1  $\mu\text{m}$ , with a uniform depth of 0.25  $\mu\text{m}$ . Wafers with a planar surface were used as controls. The silicon wafer was used as template for the production of polystyrene (PS) substrata for cell culturing. PS was solvent cast in manner described by Chesmel and Black [29]. Polystyrene replicas were attached to 18 mm diameter cylinders with polystyrene-chloroform adhesive, creating small culture dishes. Shortly before use a radio frequency glow-discharge (RFGD) treatment was applied for 5 minutes at a pressure of  $2.0 \times 10^{-2}$  mbar and a power of 200 W (Harrick Scientific Corp., Ossining, NY, USA) in order to promote cell attachment by improving the wettability of the substrata and to sterilise the culture dishes.

### *Cell culture:*

Rat dermal fibroblasts (RDF) were obtained from the ventral skin of male Wistar rats as described by Freshney [30]. Cells were cultured in  $\text{CO}_2$ -independent  $\alpha$ -MEM containing Earle's salts (Gibco, Invitrogen Corp., Paisley, Scotland), L-glutamine, 10% FCS, gentamicin (50 $\mu\text{g}/\text{ml}$ ), in an incubator set at 37  $^\circ\text{C}$  with a humidified atmosphere. Experiments were performed with 4 - 8th culture generation cells. Onto the various substrata,  $2.0 \times 10^4$  cells/ $\text{cm}^2$  were seeded. Cells were pre-cultured for 4h in the culture dishes, after which they were placed in a 12 wells plate for support. Custom-made silicone caps closed each well and the tissue culture dish therein. Using a type 22G1 needle and applying a little pressure while adding additional medium removed air bubbles. In this system with only one specific density fluid and absent air bubbles no fluid motion was to be expected, since the media was moving with the same velocity as the cell monolayer. The well plates containing the samples were inserted into aluminium culture boxes inside the centrifuge [31]. From previous studies it is known that fibroblasts need approximately 4 hours to commence adapting their morphology to a new environment [32]. Therefore experiment times were chosen of 0.5 and 2 and 4 hours to obtain information on the cells behaviour from an early time period until a state of stability between the cells and their environment.

### *Inertial shear:*

The medium size centrifuge for acceleration research (MidiCAR) was used in this study to induce inertial shear stress as has been described earlier (**Figure 2**). In short, the centrifuge is housed inside a temperature controlled cabinet and contains a control sample compartment enabling the control samples to undergo the same environmental conditions, yet at 1  $g$  (Earth) gravity. The culture dishes with a grooved substratum were placed with the grooves perpendicular to the radial

axis of rotation inside the 12-wells plate). Wells plates were placed inside a culture box which was hung in brackets inside the MidiCAR. The boxes were prevented from tilting by inserting wedges between the box top and the swivel point of the bracket. This setup results in a force parallel to the cell substratum instead of on top of the cells as in a regular swing-out centrifuge, and allows us to investigate the effects of inertial shear magnitude. Centrifuge programmed ranges were: 1 (control), 44 or 88 *g*. For calculations we presume the following “ideal” cell: half a sphere with a diameter of 10  $\mu\text{m}$ , a height of 5  $\mu\text{m}$  and a density of 1050  $\text{kg}\cdot\text{m}^{-3}$ . Contents:  $(4/3\pi r^3)/2 = 2.618 \times 10^{-16} \text{ m}^3$ . Diameter through the cell centre  $(\pi r^2)/2 = 7.854 \times 10^{-11} \text{ m}$ . Solving for cell mass we get:  $2.618 \times 10^{-16} \text{ m}^3 \times 1050 \text{ kg}\cdot\text{m}^{-3} = 2.749 \times 10^{-13} \text{ kg}$ . At 1 *g*:  $F = ma \Rightarrow 2.749 \times 10^{-13} \text{ kg} \times 9.81 \text{ ms}^{-2} = 2 \text{ pN}$ . At 44 *g* (consists of 43 *g* centrifuge program + 1 *g* Earth gravity) = 118 pN, and 88 *g* = 237 pN. These Newton values are similar to frequently used Pascal values in fluid shear force studies: if we take the cross-section of a cell (perpendicular to the surface) =  $7.854 \times 10^{-11} \text{ m}$ , then  $2.697 \times 10^{-12} \text{ N} \div 7.854 \times 10^{-11} \text{ m} = 0.0343 \text{ Pascal (N}\cdot\text{m}^{-2})$ . For 1.5 Pa follows:  $1.5 \div 0.0343 \cong 44 \text{ g}$ , for 3.0 Pa follows:  $3.0 \div 0.0343 \cong 88 \text{ g}$ .

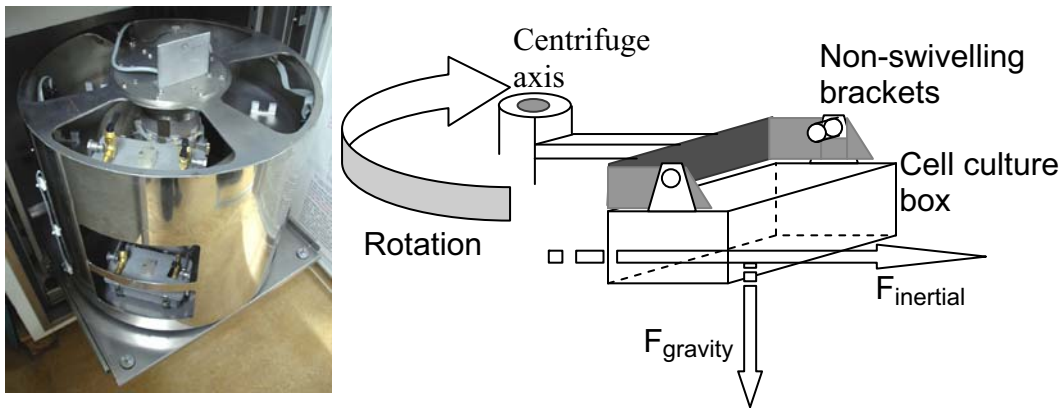


*Figure 2. The Medium Size Centrifuge for Acceleration Research (MidiCAR) used to generate inertial shear force, in which the samples were subjected up to 1, 44 or 88 times Earth’s gravity. The MidiCAR is equipped with a computerised temperature and motor control. The control samples are placed in the upper (non-spinning) compartment of the centrifuge, while the experimental samples are placed in brackets in the lower section. The brackets have wedges installed, preventing them from tilting. Graphical presentation of a secured rotating culture box, showing the direction in which inertial shear force acts on the cells.*

Similar values are used in fluid shear studies with endothelial cells [33] or for bone cells [34]. Since it has been suggested that the rate (determined by the frequency and amplitude) rather than the magnitude of the applied loading stimulus alone is more important in evoking cellular responses, an intermittent setting was applied [34]. The force was sinusoidal with a period of 12 seconds for 44 *g* and 18 seconds for 88 *g*. Immediately after the end of each experiment run, the samples were retrieved from the centrifuge and the cells were washed three times with Phosphate Buffered Saline (PBS) and prepared for further analysis.

#### *Scanning electron microscopy (SEM):*

To assess overall morphology of the fibroblasts, SEM was performed. Cells were rinsed, fixed for 5 minutes in 2% glutaraldehyde, followed by 5 minutes in 0.1 M sodium-cacodylate buffer (pH 7.4), dehydrated in a graded series of ethanol, and dried in tetramethylsilane to air. Specimens were sputter-coated with gold and examined with a JEOL 6330 Field Emission SEM (Tokyo, Japan).

#### *Immunofluorescence*

Components of the cytoskeleton were made visible using fluorescent staining techniques. RDF cells, cultured on microgrooved substrata were rinsed in PBS, pH7.2, fixed for 30 minutes in 3% paraformaldehyde/0.02% glutaraldehyde, and permeabilised with 1% Triton X100 for 5 min.

Filamentous actin was stained with Alexa Fluor 568 phalloidin (Molecular Probes, A-12380, Leiden, The Netherlands) diluted in 1% Bovine Serum Albumin/0.1% Tween-20 in PBS to block non-specific epitopes. Vinculin was stained with rabbit polyclonal primary antibodies to talin (Santa Cruz Biotechnology Inc., Santa Cruz, CA, USA), followed by labelling with goat anti-rabbit secondary antibodies IgG with Alexa Fluor 488 (Molecular Probes, A-11034) diluted in 1% BSA in PBS (1:400). Finally, the specimens were examined with a Biorad (Hercules, CA, USA) MRC 1024 confocal laser scanning microscope (CLSM) system with a krypton-argon laser at magnification of 40x. The digital immunofluorescence images acquired with the CLSM were loaded into Image J (version 1.5.0, Wayne Rasband, NIH, USA) to create overlay images. Cytoskeletal components were examined for their overall morphology as well as their orientation with respect to the groove direction. For quantitative image analysis samples were stained with Phalloidin-TRITC (Sigma, P-1951, St. Louis, MO, USA), followed by examination with a Leica/Leitz DM RBE Microscope (Wetzlar, Germany) at magnification of 10x.

### *Image Analysis*

The Phalloidin-TRITC fluorescence micrographs were analyzed with Scion Image software (Beta Version 4.0.2, Scion Corp., Frederick, MD, USA). The orientation of fibroblasts was examined and photographed. For each sample six fields of view were selected randomly. The criteria for cell selection were (1) the cell is not in contact with other cells and (2) the cell is not in contact with the image perimeter. The maximum cell diameter was measured as the longest straight line between two edges within the cell borders. The angle between this axis and the grooves (or an arbitrarily selected line for smooth surfaces) was termed the orientation angle. If the average angle was 45 degrees, cells were supposed to lie in an at random orientation. Cell extensions like filopodia, which could confound the alignment measurement, were not included when assessing the cell orientation. Using Clarks criteria [35; 36], cells oriented at 0–10 degrees from the groove direction were regarded to be aligned. The distribution of cytoskeletal patterns with time, shear force in view of the type of microgrooves and groove direction was described by the percentage of cells in the sample that displayed each pattern. Between 500 - 800 cells were measured per group. Closely linked to cell orientation: cellular surface area and cell shape ratio were also measured with the aforementioned image analysis software to obtain information on cell spreading and elongation. Applying the same criteria for cell selection; cell areas were determined and displayed as  $\mu\text{m}^2$ . Cell shape ratio were calculated as the ratio of the major to the minor dimension of a cell, by dividing the lengths of the major axis by the minor axis of the best fitting ellipse. A value of 1 corresponds to a perfect circle, while higher values correspond to more elongated cells. Between 250 - 500 cells were measured per group for orientation, area, and shape.

### *Quantitative-PCR*

Total RNA was isolated from fibroblasts with an RNA isolation and stabilisation kit (QIAGEN, Hilden, Germany) and cDNA was synthesised with reverse transcription from 2 ng aliquots of total RNA with an RT-PCR kit (Invitrogen, Carlsbad, CA, USA).

After RNA isolation, stabilisation, and cDNA amplification; 12.5  $\mu\text{l}$  of iQ SYBR Green SuperMix (Bio-Rad, Hercules, CA, USA) is added to each well of an optical 96 wells plate, 1.5  $\mu\text{l}$  of both forward and reverse primer is added, as well as, 4.5  $\mu\text{l}$  DEPC and 5  $\mu\text{l}$  of 10 times diluted cDNA sample. The wells plate is covered and centrifuged shortly to remove air bubbles, following PCR quantification using cycling parameters: 95 °C x3 min; 95 °C x15 seconds → 60 °C x30 seconds followed by 72 °C x30 seconds for 40 cycles. All samples were assayed in triplicate. The comparative Ct-values method was used to calculate the relative quantity of  $\alpha 1$ -,  $\beta 1$ -, and  $\beta 3$ -integrin, and Collagen Type I and glyceraldehyde-3-phosphate dehydrogenase (GAPDH).

Expression of the housekeeping gene (GAPDH) was used as an internal control to normalise results [37].

#### *SDS-PAGE and Western Blot analysis*

For preparing total protein extracts; cells were washed 3 times with ice cold PBS. Cells were harvested by scraping followed by disruption with 500  $\mu$ l ice-cold lysis buffer (50 mM Tris (pH 7.4), 250 mM NaCl, 5 mM EDTA, 50 mM NaF, 1mM Na<sub>3</sub>VO<sub>4</sub>, 1% Nonidet P40 (BioSource, Camarillo, CA, USA) supplemented with 1 mM Phenylmethanesulfonyl fluoride (PMSF, P7626, Sigma-Aldrich, Steinheim, Germany) and Protease Inhibitor Cocktail (P2714, Sigma-Aldrich). Samples were cleared of cellular debris and concentrated by centrifugation for 65 minutes, 4°C at 12,000 rpm (Amicon Microcon YM-10 centrifugal filter tube, Millipore, Billerica, MA, USA). The protein concentrations in the retentate were determined, and equal amounts of protein were dissolved in 10 $\mu$ l of 2x reducing sample buffer (4% SDS, 100mM Tris (pH 6.0), 10%  $\beta$ -mercaptoethanol, 20% Glycerol) and heated at 95°C for 5 minutes and electrophoresed on 12.5% SDS-Acrylamide minislab gels and transferred to (polyvinylidene difluoride) PVDF membranes (Immobilon-P, Millipore). After protein transfer, the membranes were blocked in 4% skim milk in TBST (0.05% Tween 20 in TBS) overnight at room temperature. Immunological blots were then performed at room temperature for 1 hour in 2% skim milk in TBST buffer containing specific primary antibodies.

#### *Antibodies for Western Blot analysis*

Western blots were probed with the following antibodies: Anti-ERK 1/2 (C-16; sc-93), JNK1 (C-17; sc-474), p38 MAPK (C-20; sc-535),  $\alpha$ PAK (H-300; sc-11394), RhoA (119; sc-179), Rac1 (T-17; sc-6084), Cdc42 (P1; sc-87). Anti-active p-ERK 1/2 (E-4; sc-7383), p-JNK (G-7; sc-6254), p-p38 (D-8; sc-7973). All antibodies were obtained from Santa Cruz Biotechnology .

After membranes were washed with TBST, they were incubated with appropriate secondary antibody IgG with alkaline phosphatase conjugate and immuno-reactive bands were visualized using Nitroblue Tetrazolium (NBT) and 5-bromo-4-chloro-3-indolyl phosphate (BCIP) chemiluminescence reagents (Bio-Rad Laboratories Hercules, CA, USA).

#### *Statistical analysis:*

Acquired data from the fluorescence micrographs on cell alignment and QPCR data were analysed using SPSS for Windows (Release 12.0.1, SPSS Inc., Chicago, USA). The effects of and the interaction between both time and/or force and surface were analysed using analysis of variance (ANOVA), including a modified least significant difference (Tukey) multiple range test to detect significant differences between two distinct groups. Probability (p) values of  $\leq 0.05$  were considered significant.

## **RESULTS**

### *Scanning electron microscopy*

The micro topography pattern of grooves and ridges was accurately reproduced in the polystyrene substrata, down to the nano roughness along the edges of the ridges (data not shown). When examining cell morphology, RDFs cultured on smooth substrata showed a recognisable cell spreading associated with the early stages of cell adherence: from round cells with abundant amounts of filopodia to flat outstretched cells with large cell surface areas. The spreading pattern itself is considered random, since common cellular orientation could not be distinguished (**Figure 3A-C**). RDFs seeded onto grooved substrata already demonstrated orientation along the grooves from an early time point onward although their cell bodies were still rather wide. Since the

groove/ridge pitch is too small for the cells to descend to the bottom of the grooves they were always found on top of the ridges. Cellular extensions probing the substratum surface only find the top ridge, resulting in extension of the cellular body along these small ridges. In later stages the fibroblasts had stretched out themselves into elongated cells with narrow cell width and are highly aligned (**Figure 3D-F**).

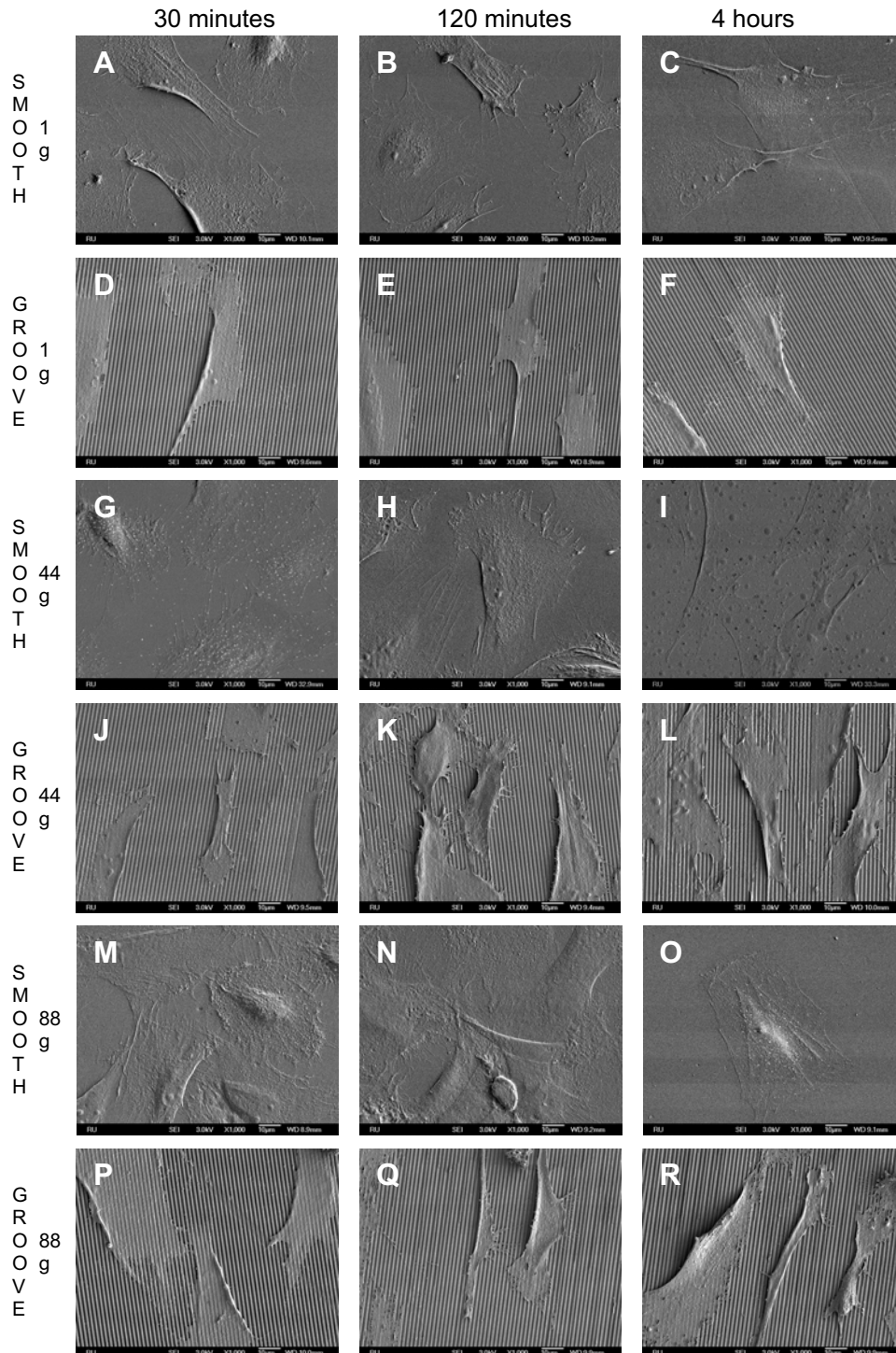


*Figure 3. SEM micrographs of RDFs cultured under various conditions. Columns represent time; from left to right: 0.5, 2 and 4 hours. Rows represent a combination of topography and amount of shear force applied. First two rows: 1 g, Smooth and Grooved. Next two rows: 44 g, last two rows: 88 g (magnification x1000).*

When subjected to inertial shear force, RDFs cultured on smooth topography remained morphologically quite similar compared to controls (**Figure 3G, H, M, & N**): round cells with numerous filopodia at the early stages. After 4 hours fibroblasts appeared as long, flat, shaped cells (**Figure 3I, O**). RDFs seeded onto grooved surface exposed to 44 g intermittent shear appeared

dissimilar in their cell morphology when compared to their 1 *g* counterparts (**Figure 3J-L**). Fibroblast after 2 and 4 hours of experiencing shear stress had heightened cell bodies and displayed membrane ruffles. Cellular morphology under 44 *g* resulted in cells appearing less orientated along the grooves on the whole, displaying membrane ruffles, and many filopodia stretching in all directions. Also cell surface area seems larger, due to wider cell bodies. When subjected to 88 *g* (**Figure 3P-R**), fibroblasts at first display wide cell bodies, but gradually became more narrow and more aligned compared to their control group.

#### *Fluorescence microscopy*

The cytoskeleton was investigated by staining filamentous actin and talin anchor points of the cell focal adhesions. **Figure 4A-C** shows 1 *g* smooth substratum samples for 3 time points; the observed cell shape, spreading, and random orientation were comparable to SEM micrographs. F-actin filaments (red staining) were running in the direction of not only the long axis of cells, but also around the cell membrane, and crossing over the cell nucleus. Talin (green) for focal adhesions resulted in a staining around the nucleus, and talin spots were visible in some samples, positioned at the end of actin bundles, and always extended in the direction of the actin bundle. RDFs cultured on grooved surfaces displayed a comparable morphology with SEM, however, there seems to be a more pronounced orientation of the cells and their cytoskeleton in time (**Figure 4D-F**). Cells are most stretched out and slender after 2 hours of culturing. Before that, cells are rounder and after 4 hours still aligned, yet their cell bodies were wider.

In **Figure 4G, H, & I**, RDFs can be observed cultured on a smooth surfaces and subjected to 44 *g* intermittent inertial shear force. It was striking that the actin filaments appeared thicker and more numerous. In addition, cells were not as round as one would expect during these early time points. After 4 hours, they displayed abundant actin filaments, not only in the direction of the long axis, but also perpendicular to the axis. Fibroblasts on grooved substrates experiencing 44 *g* inertial shear force displayed a shape and alignment pattern as observed within the control group (**Figure 4J-L**).

In contrast to the 44 *g* inertial shear force, 88 *g* resulted in cells, cultured on smooth substrates, remaining their round shape for a longer period (**Figure 4M, N**). After 4 hours of intermittent shear force, cells display a disturbed cytoskeleton; actin filaments were thin, albeit abundant, and talin anchor points are reduced in number and seemed to concentrate around the cell nucleus (**Figure 4O**). Copious amounts of actin filaments were seen in RDFs seeded onto grooved substrata experiencing 88 *g*. They seemed to be able to stay aligned, although after 4 hours the orientation along the grooves seemed to decrease, comparable to the other experiment and control group. The focal anchor points as visualised by the talin immuno-staining were predominantly centered around the cell core (**Figure 4P-R**).

#### *Image analysis*

The actin filaments stained with Phalloidin-TRITC were plainly visible and fibroblast cellular orientation corroborated with the SEM: RDFs cultured on grooved substrata displayed alignment along the ridges, while smooth surfaces did not bring about any form of alignment. The quantified results for cell orientation are presented as mean angle and standard error of the mean in **Figure 5**. Averaging around 45 degrees, smooth substrata did not induce any cellular orientation compared to their grooved equivalents, which, all groups combined, averaged around 12 degrees. Within the smooth groups no significant change in mean angle occurred, however, differences were observed among the various grooved substrate groups. Most striking was the significant decrease in mean angle (thus an increase in alignment) after 2 hours and the increase in mean angle at 4 hours. This reoccurring pattern took place in all groups.

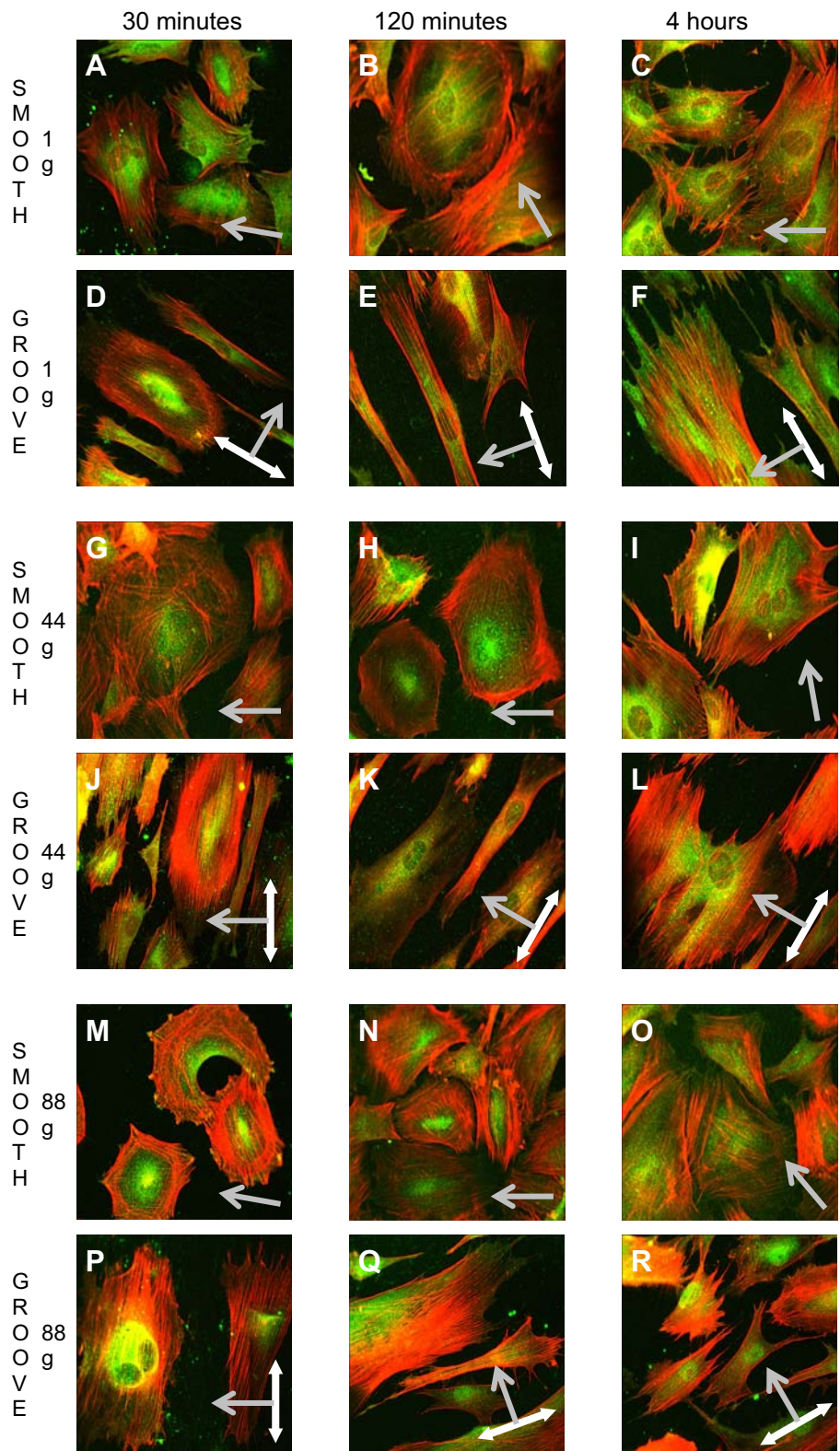


Figure 4. CLSM micrographs of RDFs cultured under several conditions. Columns represent time; from left to right: 30, 120 minutes and 4 hours. Rows represent a combination of topography and amount of shear force applied. First two rows 1 g, Smooth and Grooved. Next two rows: 44 g, last two rows: 88 g. Double ended white arrow denotes groove direction, single grey arrow denotes shear direction. Colour figure on page 166.

Analysis of variance multiple comparison test (ANOVA) analysis of the main parameters: topography, inertial shear force, and time all proved significant. Regarding topography; combining all groups: 65% of the cells were aligned along the grooved substrata compared to 13% on smooth substrata. Inertial shear force significantly influences cellular orientation along grooved surfaces: 44 g resulted in a higher mean angle and a reduced total number of cells matching the alignment criteria (average: 16 degrees for 53% of the cells) compared to the control and 88 g groups,

respectively 10° - 70%, and 13° - 68%. Finally, the effects of time on fibroblast orientation was significant in all 2 hours sample groups showing a higher percentage of cells aligned and a subsequent lower mean angle independently of the inertial shear force applied. On the whole, within the grooved 2 hours group; 75% of the cells aligned to around 9°, compared to 16°- 56% (30 min group) and 14° - 59% (4 hours experiment group).

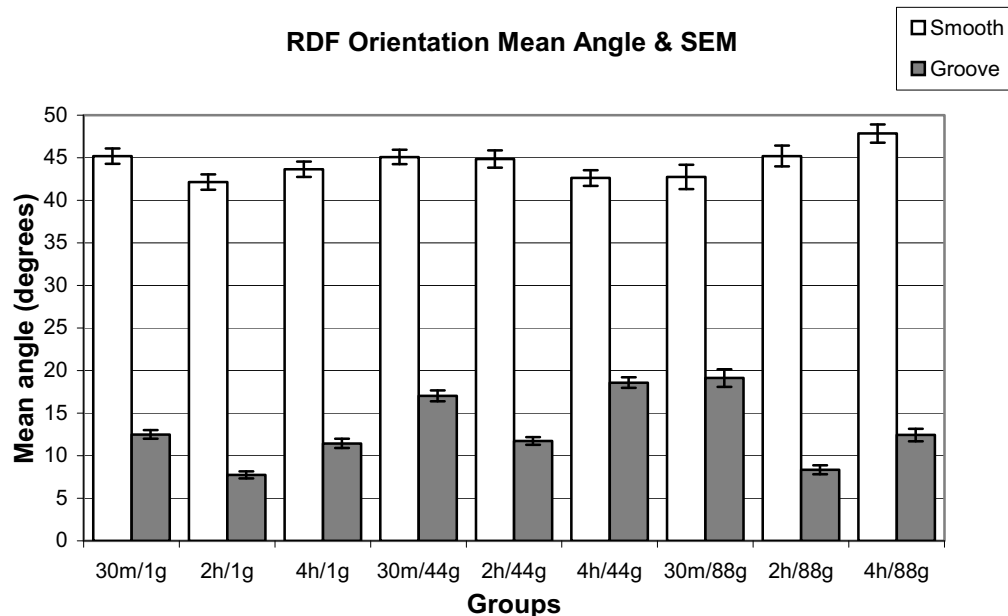


Figure 5. Bar graphs showing the distribution of cellular orientation of fibroblasts under various circumstances of inertial shear. Smooth substrata results in random spread of cells, as indicated by a mean angle around 45 degrees for all experiment groups. Grooved surfaces elicit cellular alignment. The lowest mean angle is reached after 2 hours of culturing, after which a slight increase happens. For each sample at least 500 individual cells were analysed. 30m, 2h and 4h stands for the experiment time, and 1, 44, and 88 g stands for the applied inertial shear force.

Cell surface area measurements revealed an interesting cellular response of fibroblasts towards shear stress (Figure 6). On smooth substrates non loaded cells appeared round (30 minutes) and gradually became more spindle shaped (4 hours), their overall cell area averaged around 2900  $\mu\text{m}^2$ . However, from 4 hours at 44 g onward, cell surface area jumps to 5307  $\mu\text{m}^2$  and remains at this level throughout 88 g groups. While smooth 4 hr/44 g still had spindle shaped cells, their cell bodies are wider with more protrusions compared to their 4 hr/1 g counterparts. Fibroblasts exposed to 88 g had a round shape and never attained a spindle shape. Cells cultured on a grooved substrate had an overall cell surface area between 1600-2100  $\mu\text{m}^2$  (1 and 44 g groups only). Cells cultured for 4 hours were in the high end of this range. A significant increase in cell area was measured in the 88 g groups: cells exposed to 88 g for 30 minutes had areas of 2704  $\mu\text{m}^2$ . After 4 hours at 88 g this had increased to 3575  $\mu\text{m}^2$ .

Finally, cell shape ratios were calculated to investigate fibroblast elongation (Figure 7). Under normal gravity circumstances fibroblast cultured on grooved surface had higher ratios compared to cells cultured on smooth surfaces. Thus, their cell bodies were more elongated/ellipse shaped. During both 44 and 88 g within the smooth groups there is a small, yet significant rise in shape ratio when comparing 30 minutes and 4 hours. Within the grooved group a significant peak is measured at 2 hours, followed by a decrease at 4 hours. The higher absolute ratios after 2 and 4 hours within the 88 g group compared to their 44 g counterparts proved to be no more than a trend.

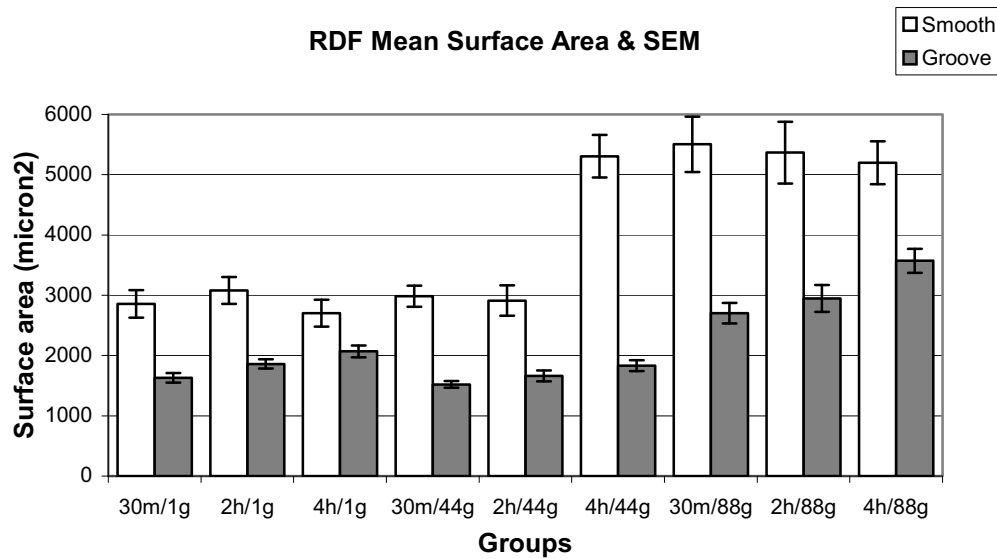


Figure 6. Bar graphs showing the mean and standard error of the mean for cell surface area of fibroblasts subjected to various conditions. S = smooth, G = grooved, 30m, 2h, and 4h stands for the experiment time, and 1, 44, and 88 g stands for the applied inertial shear force. For each sample at least 250 individual cells were analysed.

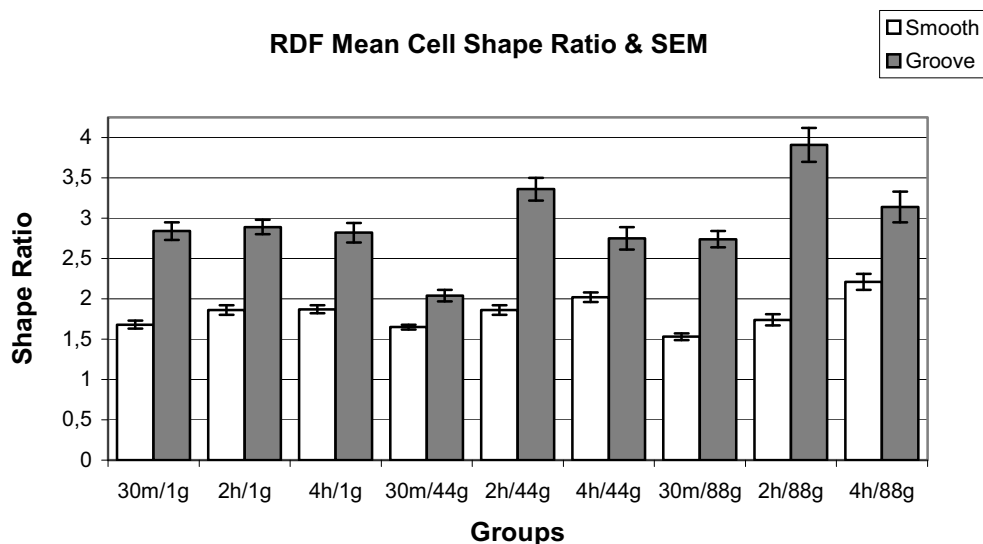


Figure 7. Bar graphs showing the mean and standard error of the mean for cell shape ratio of fibroblasts subjected to various conditions. S = smooth, G = grooved, 30m, 2h, and 4h stands for the experiment time, and 1, 44, and 88 g stands for the applied inertial shear force. For each sample at least 250 individual cells were analysed.

### Quantitative-PCR

Real-time PCR analysis was conducted to quantify mRNA expression of  $\alpha 1$ ,  $\beta 1$ - and  $\beta 3$ -integrins, and collagen type I. **Table 1** shows the amounts of the various transcripts relative to GAPDH, and data were normalised to the expression of the genes of interest in the respective control (1 g) groups (so called  $2^{-\Delta\Delta CT}$  method).

Expression of these proteins, which are involved in the cellular interface with the environment, were influenced by both time and inertial shear force independently, even though both parameters interacted with each other. The latter remark was clearly visible in the 4 hours groups.

On the whole, fibroblast cultured on smooth surfaces which received 88 *g* of shear force responded much stronger than those cells cultured on grooved surfaces undergoing the same force. Alpha-1, beta-1, and beta-3 integrin expression was severely reduced in all but the 4 hours experiment groups. In those groups a significant up-regulation was shown, particularly by fibroblast cultured in smooth substrata en being subjected to 88 *g* of shear force. Of the three integrins, beta-1 integrin responded most intensely to both time and inertial shear, the relative mRNA levels were highest after 4 hours. Collagen type I revealed an up-regulation after 30 minutes and at 4 hours, while after 2 hours a significant down-regulation was seen. The sole exception being the 88 *g* groove group which showed an increase at 2 hours, but none at 4 hours.

Groups	alpha-1	beta-1	beta-3	collagen I
S 30m 44g	0.5 (0,4-0,6)	0.6 (0,5-0,9)	0.6 (0,4-0,7)	<b>3.6</b> (2,4-5,5)
S 2h 44g	0.2 (0,2-0,4)	0.5 (0,3-0,9)	0.2 (0,1-0,4)	0.6 (0,4-0,9)
S 4h 44g	<b>5.0</b> (2,2-11,2)	<b>3.2</b> (1,7-6,1)	<b>4.2</b> (2,1-8,3)	0.2 (0,1-0,4)
S 30m 88g	0.5 (0,3-0,7)	1.0 (0,6-1,6)	0.5 (0,3-0,8)	1.5 (1,1-2,0)
S 2h 88g	0.7 (0,4-1,1)	0.8 (0,5-1,5)	0.5 (0,3-0,9)	0.3 (0,2-0,5)
S 4h 88g	<b>12.4</b> (5,4-28,5)	<b>5.6</b> (2,9-11,1)	<b>11.7</b> (5,5-24,8)	0.4 (0,2-0,9)
G 30m 1g	0,1 (0,0-0,9)	0,9 (0,2-3,1)	0,3 (0,1-1,2)	1,7 (0,8-4,5)
G 2h 1g	0,1 (0,0-0,5)	0,2 (0,1-0,9)	0,2 (0,1-0,7)	0,5 (0,2-1,0)
G 4h 1g	1,6 (0,2-10,3)	<b>6,2</b> (1,5-25,8)	<b>3,5</b> (0,7-17,9)	0,9 (0,4-2,3)
G 30m 44g	0,5 (0,2-1,1)	0,9 (0,4-2,2)	0,6 (0,2-1,8)	2,2 (1,1-4,2)
G 2h 44g	0,2 (0,1-0,4)	0,4 (0,2-0,6)	0,2 (0,1-0,3)	0,4 (0,2-0,6)
G 4h 44g	<b>5,7</b> (2,5-13,0)	<b>5,5</b> (3,2-9,2)	<b>3,0</b> (1,4-6,5)	0,4 (0,2-0,9)
G 30m 88g	0,5 (0,5-0,7)	0,8 (0,7-0,9)	0,3 (0,3-0,3)	2,1 (1,4-3,2)
G 2h 88g	0,1 (0,0-0,3)	0,2 (0,1-0,4)	0,3 (0,2-0,5)	<b>4,0</b> (2,4-6,6)
G 4h 88g	<b>6,6</b> (4,5-9,8)	<b>8,1</b> (5,4-12,1)	<b>6,5</b> (4,5-9,6)	0,1 (0,1-0,2)

Table 1. *Effects of surface, time, and shear force on the relative gene expression of alpha-1, beta-1, beta-3-integrins, and collagen type I was analysed by quantitative PCR. Data are expressed as 2<sup>ΔΔCT</sup> and range, n = 4. Values were relative to internal control gene GAPDH and normalised to Smooth 1g. Significantly different samples (p < 0.05) are in bold face.*

#### Immunoblot analysis

Western blot analysis showed that within the Mitogen Activated Protein Kinase (MAPK) pathways, all three major signalling pathways were present: ERK-1/2, JNK/SAPK-1/2, and p38<sup>MAPK</sup>. The presence of both total and active protein could be detected (**Figure 8 A-C**). ERK-1/2 protein appeared in all groups, especially ERK-1 was clearly up-regulated at 30 and 120 minutes within the grooved groups. Phosphorylated (active) Erk-1/2 is most present in the early stages, and seemed to be particularly increased at the control groups and the 88 *g* groups, be it grooved or smooth. JNK-1/2 and p38<sup>MAPK</sup> presence was evenly distributed within the groups. Their active components appeared most strongly in those groups which are subjected to 44 *g* inertial shear. Although p-JNK and p-p38 emerge throughout the different time points, they most often displayed more obvious bands at earlier (30 and 120 minutes) measurements.

In addition to the three pathways, several proteins which play essential roles in cellular attachment to and movement across substrates were investigated. RhoA, an upstream element of the ERK pathway, was found to be present under inertial shear conditions independently from surface topography (**Figure 9A**). Together with its downstream effector ROCK1/2, RhoA induces actin stress fibres and focal-adhesion complexes, to which the ends of the stress fibres attach. Upstream of the JNK/SAPK pathway and intimately linked to RhoA, are Cdc42 and Rac1. These two proteins stimulate the formation of Cdc42 induced filopodia with Rac1 induced membrane ruffles leading to cell movement. Cdc42 was found in both topographical groups, and appears to be continuously up-regulated within the fibroblast. The Rac1 fusion protein too was present in the various experiment groups. Larger bands of this protein were visible in the static control groups and the early time points (30 minutes) of the experiment groups (**Figure 9B, C**).

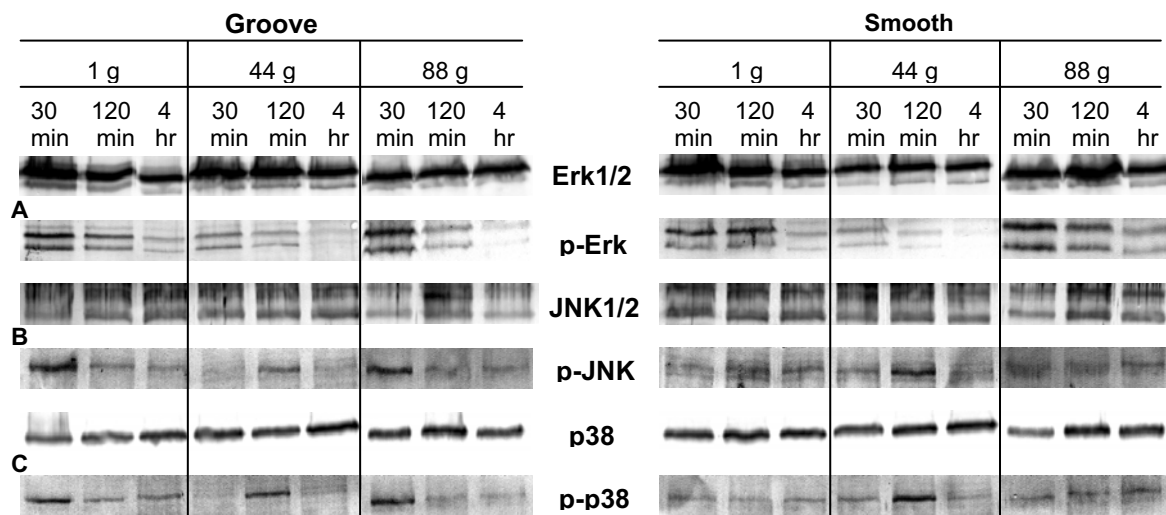


Figure 8. Western blots analysis of MAPK signalling pathways from whole cell lysates prepared from primary fibroblasts. Equal amount of protein were probed with antibodies specific to total ERK1/2 (A, top row) and phospho-ERK1/2 (A, bottom row) followed by immuno-staining with IgA Alkaline Phosphate conjugate. The whole cell extracts as described in panel A were analyzed by Western blotting. Samples were probed with antibodies specific for total JNK1/2 (B, top row) and phospho-JNK1/2 (B, bottom row), total p38 (C, top row) and phospho-p38 (C, bottom row).

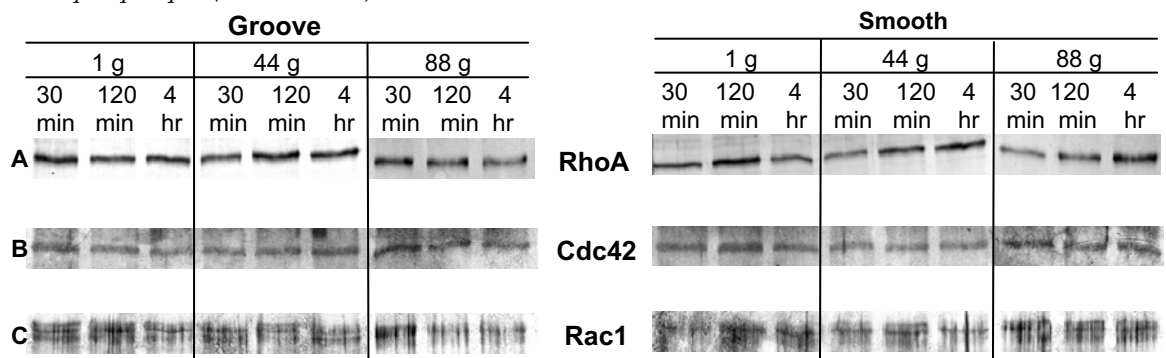


Figure 9. Western blots analysis of small GTPases family members from whole cell extracts prepared from primary fibroblasts. Equal amount of protein were probed with antibodies specific to total RhoA (A), Cdc42 (B), Rac1 fusion protein (C), followed by immuno-staining with IgA Alkaline Phosphate conjugate. The whole cell extracts were analyzed by Western blotting.

## Discussion

In this *in vitro* study we shed, for the first time, some light on the magnitude of inertial shear forces on fibroblast cells cultured on both smooth and microgrooved polystyrene substrata placed inside a centrifuge setting. The underlying aim was to understand to what extent shear forces can alter cell behaviour and if inertial shear could be utilized as a model to explain possible phenomena as found in experiments which use centrifuges to investigate mechanotransduction in mammalian cells, particularly to study the signalling mechanisms and stress responses. The mechanotransduction of these static and dynamic forces transferred onto the cells were investigated: morphological cell responses like shape and orientation and related to that the cytoskeleton of the cells; the expression of several proteins involved in cell-surface interaction by means of Q-PCR were also investigated. Finally, proteins of the MAPK intracellular signalling kinase pathways were visualised. From our data we concluded that fibroblast adjust their shape according to micro-topographical features. Even so, inertial shear force plays a significant role in the response by RDFs to external loads. Although cells, in relation to their morphology, have a tendency to rely more on the static stresses encountered from the substratum, cellular behaviour

on a molecular level (i.e. mRNA transcripts and intracellular signalling pathways), as well as, whole cell colony performance are markedly influenced by inertial shear force.

Adherent cells will experience a large inertial shear acceleration and will lead to cell deformation (strain). In our study this strain on individual cells is visible as cells appearing less aligned along the microgrooves. The cell surface in general has increased, signalling the probability of fibroblasts forming stable attachments in order to withstand the inertial shear force better. Combined with the polymerization of abundant thicker actin filament bundles in the long axis of the fibroblast, but also in the short axis points to fibroblast able to sense inertial shear and respond to it in such a way as to minimize the stress on their cytoskeleton. In initial observation we noted a displacement of large numbers of cells towards the outer limits of the culture dish might indicate that even minimum low levels of shear force can relocate the bulk of the cell colony.

Inertial shear stress as a cell body force model to study mechanical and biological responses of cells is useful in understanding activation of the various pathways after mechanical stimulus. Explicitly, the model can identify the region within which forces or deformations are of sufficient magnitude to potentially elicit a biological response. Currently, much is known about the signalling pathways that are initiated when cells are subjected to a mechanical stress. However the process of mechanotransduction by which the mechanical disturbance is transformed into a biochemical signal is poorly understood.

The inertial shear force paradigm could possibly aid in linking mechanotransduction phenomena to mechanically-induced alterations in the molecular conformation of proteins [38]. These changes in conformation can lead to altered binding affinities of proteins, and ultimately initiating an intracellular signalling cascade or lead to changes in the proteins localized to regions of high stress. This hypothesis represents an alternative to transmembrane signalling via receptor-ligand interactions providing the cell with a means of reacting to changes in its mechanical, as opposed to biochemical, environment. By applying inertial shear as means to study conformational changes in the load-bearing regions of focal adhesion complexes for instance or the cytoskeleton, a more general quantitative description of mechanotransduction pathways should be possible [17; 39-43]. Fibroblasts are clearly affected by inertial shear force; their morphology under normal and shear conditions are markedly different. Cells subjected to shear display many filopodia, membrane ruffles, and thinner actin filaments, this corresponds with the up-regulation of beta-1 integrin, and the down-regulation of beta-3. Integrin recycling regulates cell migration, and especially beta-3 recycling influences the cell's decision to migrate with persistence or to move randomly [44] [45]. The displacement/migration of a substantial part of the cell colony to the outer rim of the culture dish away from the inertial shear force, and the continuous presence of both Cdc42 and Rac1 fusion protein are signs that cell body forces assert their stress onto the cellular structures [39]. JNK/SAPK and p38<sup>MAPK</sup>, proteins which are activated downstream of the Rac1/Cdc42, are present within the shear experiment groups, combined with the reduction in Erk1/2. Thus, it appears cells are under significant stress and are sensitized to apoptosis via the up-regulation of p38 and the reduced regulation of survival pathways [46; 47]. Nonetheless, Erk1/2 is still largely present and so is RhoA. Fibroblasts obviously are trying to manage the situation created by inertial shear force. With Erk1/2, a survival pathway, up-regulated, and the strong presence of RhoA, which mediates the formation and maturation of focal adhesion complexes on the basal surface of the cell, fibroblasts sense the stress and are active in achieving a state of mechanical equilibrium (balance of forces). The cytoskeleton near the cortical surface does not necessarily sense the same stress. This hypothesis is supported by related studies that show release of prostaglandins in response to fluid shear stress being mediated by focal adhesion, and proteoglycans in the glycocalyx (associated plasma proteins of glycosaminoglycans) that have a transmembrane domain that can interact with the apical cytoskeleton [43; 48]. Key issue in adherent cellular survival is

the presence of extracellular matrix components and a means to interact. From previous research we have learned that fibronectin and collagen type I are unaffected by hypergravity [45]. Although integrins are down-regulated in the short run, up-regulation at 4 hours onwards safeguards the cells survival in the long run. Prolonged culturing (24 - 48 hours) will most likely lead to an augmentation of mechanical equilibrium between the cell and its environment.

## CONCLUSIONS

In conclusion, we might state that topography emerges as the more dominant parameter for cellular response. However, adaptations of the cytoskeleton, the presence of intracellular proteins, and overall cell morphology point towards a competition between static and dynamic forces and results in an active cell response. A combination of inertial shear force and a nano-scale grooved pattern with longer culture times will elucidate to what extend each parameter can assert its influence on cell behaviour. This novel concept of inertial shear force is an appropriate and straightforward model to apply body forces onto cells.

## REFERENCES

1. Zhang, W., Liu, Y., and Kassab, G. S. Flow-induced shear strain in intima of porcine coronary arteries. *J Appl Physiol* 2007, 2007.
2. Park, S. W., Byun, D., Bae, Y. M., Choi, B. H., Park, S. H., Kim, B., and Cho, S. I. Effects of fluid flow on voltage-dependent calcium channels in rat vascular myocytes: Fluid flow as a shear stress and a source of artifacts during patch-clamp studies. *Biochem Biophys Res Commun* 2007, 1021-7, 2007.
3. Meng, H., Wang, Z., Hoi, Y., Gao, L., Metaxa, E., Swartz, D. D., and Kolega, J. Complex hemodynamics at the apex of an arterial bifurcation induces vascular remodeling resembling cerebral aneurysm initiation. *Stroke* 2007, 1924-31, 2007.
4. Schneider, S. W., Nuschele, S., Wixforth, A., Gorzelanny, C., Alexander-Katz, A., Netz, R. R., and Schneider, M. F. Shear-induced unfolding triggers adhesion of von Willebrand factor fibers. *Proc Natl Acad Sci U S A* 2007, 7899-903, 2007.
5. Zernicke, R., MacKay, C., and Lorincz, C. Mechanisms of bone remodeling during weight-bearing exercise. *Appl Physiol Nutr Metab* 2006, 655-60, 2006.
6. McGarry, J. G., Klein-Nulend, J., and Prendergast, P. J. The effect of cytoskeletal disruption on pulsatile fluid flow-induced nitric oxide and prostaglandin E2 release in osteocytes and osteoblasts. *Biochem Biophys Res Commun* 2005, 341-8, 2005.
7. Klein-Nulend, J., Bacabac, R. G., and Mullender, M. G. Mechanobiology of bone tissue. *Pathol Biol (Paris)* 2005, 576-80, 2005.
8. Brown, T. D. Techniques for mechanical stimulation of cells in vitro: a review. *J Biomech* 2000, 3-14, 2000.
9. Nerem, R. M. Shear force and its effect on cell structure and function. *ASGSB Bull* 1991, 87-94, 1991.
10. Traub, O. and Berk, B. C. Laminar shear stress: mechanisms by which endothelial cells transduce an atheroprotective force. *Arterioscler Thromb Vasc Biol* 1998, 677-685, 1998.
11. Helmke, B. P. and Davies, P. F. The cytoskeleton under external fluid mechanical forces: hemodynamic forces acting on the endothelium. *Ann Biomed Eng* 2002, 284-296, 2002.
12. Helmke, B. P., Goldman, R. D., and Davies, P. F. Rapid displacement of vimentin intermediate filaments in living endothelial cells exposed to flow. *Circ Res* 2000, 745-752, 2000.
13. Shyy, J. Y. and Chien, S. Role of integrins in endothelial mechanosensing of shear stress. *Circ Res* 2002, 769-775,

- 2002.
14. Marschel, P. and Schmid-Schonbein, G. W. Control of fluid shear response in circulating leukocytes by integrins. *Ann Biomed Eng* 2002, 333-343, 2002.
  15. Traub, O., Ishida, T., Ishida, M., Tupper, J. C., and Berk, B. C. Shear stress-mediated extracellular signal-regulated kinase activation is regulated by sodium in endothelial cells. Potential role for a voltage-dependent sodium channel. *J Biol Chem* 1999, 274:20144-20150, 1999.
  16. van Loon, J. J., Folgering, E. H., Bouten, C. V., Veldhuijzen, J. P., and Smit, T. H. Inertial shear forces and the use of centrifuges in gravity research. What is the proper control? *J Biomech Eng* 2003, 342-346, 2003.
  17. Kaazempur-Mofrad, M. R., Abdul-Rahim, N. A., Karcher, H., Mack, P. J., Yap, B., and Kamm, R. D. Exploring the molecular basis for mechanosensation, signal transduction, and cytoskeletal remodeling. *Acta Biomater* 2005, 281-293, 2005.
  18. Lee, D. J., Rosenfeldt, H., and Grinnell, F. Activation of ERK and p38 MAP kinases in human fibroblasts during collagen matrix contraction. *Exp Cell Res* 2000, 260:190-7, 2000.
  19. Wang, J. G., Miyazu, M., Matsushita, E., Sokabe, M., and Naruse, K. Uniaxial cyclic stretch induces focal adhesion kinase (FAK) tyrosine phosphorylation followed by mitogen-activated protein kinase (MAPK) activation. *Biochem Biophys Res Commun* 2001, 278:356-61, 2001.
  20. Howe, A. K., Aplin, A. E., and Juliano, R. L. Anchorage-dependent ERK signaling--mechanisms and consequences. *Curr Opin Genet Dev* 2002, 12:30-5, 2002.
  21. Aplin, A. E. and Juliano, R. L. Integrin and cytoskeletal regulation of growth factor signaling to the MAP kinase pathway. *J Cell Sci* 1999, 112:695-706, 1999.
  22. Yuge, L., Hide, I., Kumagai, T., Kumei, Y., Takeda, S., Kanno, M., Sugiyama, M., and Kataoka, K. Cell differentiation and p38(MAPK) cascade are inhibited in human osteoblasts cultured in a three-dimensional clinostat. *In Vitro Cell Dev Biol Anim* 2003, 39:89-97, 2003.
  23. Nebreda, A. R. and Porras, A. p38 MAP kinases: beyond the stress response. *Trends Biochem Sci* 2000, 25:257-260, 2000.
  24. Tang, Y., Yu, J., and Field, J. Signals from the Ras, Rac, and Rho GTPases converge on the Pak protein kinase in Rat-1 fibroblasts. *Mol Cell Biol* 1999, 19:1881-1891, 1999.
  25. He, H., Pannequin, J., Tantiogco, J. P., Shulkes, A., and Baldwin, G. S. Glycine-extended gastrin stimulates cell proliferation and migration through a Rho- and ROCK-dependent pathway, not a Rac/Cdc42-dependent pathway. *Am J Physiol Gastrointest Liver Physiol* 2005, 289:G478-488, 2005.
  26. Lim, L., Manser, E., Leung, T., and Hall, C. Regulation of phosphorylation pathways by p21 GTPases. The p21 Ras-related Rho subfamily and its role in phosphorylation signalling pathways. *Eur J Biochem* 1996, 238:171-185, 1996.
  27. Manser, E. Small GTPases take the stage. *Dev Cell* 2002, 3:323-328, 2002.
  28. Walboomers, X. F., Croes, H. J., Ginsel, L. A., and Jansen, J. A. Growth behavior of fibroblasts on microgrooved polystyrene. *Biomaterials* 1998, 19:1861-1868, 1998.
  29. Chesmel, K. D. and Black, J. Cellular responses to chemical and morphologic aspects of biomaterial surfaces. I. A novel in vitro model system. *J Biomed Mater Res* 1995, 29:1089-1099, 1995.
  30. Freshney, R. I. Culture of animal cells: a multimedia guide. 99. Chichester, John Wiley & Sons Ltd.
  31. van Loon, J. J., van den Bergh, L. C., Veldhuijzen, J. P., and Huijser, R. Development of a centrifuge for

- acceleration research in cell and developmental biology. In academic thesis: Effect of spaceflight and hypergravity on mineral metabolism in organ cultures of fetal mouse long bones. Appendix C. 95. Amsterdam, Free University Amsterdam.
32. Walboomers, X. F., Ginsel, L. A., and Jansen, J. A. Early spreading events of fibroblasts on microgrooved substrates. *J Biomed Mater Res* 2000, 529-534, 2000.
  33. Patrick, C. W., Sampath, R., and McIntire, L. V. Fluid Shear Stress Effects on Cellular Function. 1626-1645. 95. CRC Press Inc. Biomedical Research Handbook: Tissue Engineering Section. B. Palsson and J.A. Hubbell.
  34. Bacabac, R. G., Smit, T. H., Mullender, M. G., Van Loon, J. J., and Klein-Nulend, J. Initial stress-kick is required for fluid shear stress-induced rate dependent activation of bone cells. *Ann Biomed Eng* 2005, 104-110, 2005.
  35. Clark, P., Connolly, P., Curtis, A. S., Dow, J. A., and Wilkinson, C. D. Topographical control of cell behaviour: II. Multiple grooved substrata. *Development* 1990, 635-644, 1990.
  36. Clark, P., Connolly, P., Curtis, A. S., Dow, J. A., and Wilkinson, C. D. Topographical control of cell behaviour. I. Simple step cues. *Development* 1987, 439-448, 1987.
  37. Livak, K. J. and Schmittgen, T. D. Analysis of relative gene expression data using real-time quantitative PCR and the 2(-Delta Delta C(T)) Method. *Methods* 2001, 402-8, 2001.
  38. van Loon, J. J. W. A. Micro-gravity and mechanomics. *Gravitational and Space Biology* 20(2), 3-18. 2007.
  39. Tarbell, J. M., Weinbaum, S., and Kamm, R. D. Cellular fluid mechanics and mechanotransduction. *Ann Biomed Eng* 2005, 1719-1723, 2005.
  40. Lemmon, C. A., Sniadecki, N. J., Ruiz, S. A., Tan, J. L., Romer, L. H., and Chen, C. S. Shear force at the cell-matrix interface: enhanced analysis for microfabricated post array detectors. *Mech Chem Biosyst* 2005, 1-16, 2005.
  41. Karcher, H., Lammerding, J., Huang, H., Lee, R. T., Kamm, R. D., and Kaazempur-Mofrad, M. R. A three-dimensional viscoelastic model for cell deformation with experimental verification. *Biophys J* 2003, 3336-3349, 2003.
  42. Kamm, R. D. and Kaazempur-Mofrad, M. R. On the molecular basis for mechanotransduction. *Mech Chem Biosyst* 2004, 201-209, 2004.
  43. Norvell, S. M., Ponik, S. M., Bowen, D. K., Gerard, R., and Pavalko, F. M. Fluid shear stress induction of COX-2 protein and prostaglandin release in cultured MC3T3-E1 osteoblasts does not require intact microfilaments or microtubules. *J Appl Physiol* 2004, 957-966, 2004.
  44. White, D. P., Caswell, P. T., and Norman, J. C.  $\alpha_v\beta_3$  and  $\alpha_5\beta_1$  integrin recycling pathways dictate downstream Rho kinase signaling to regulate persistent cell migration. *J Cell Biol* 2007, 515-525, 2007.
  45. Loesberg, W. A., Walboomers, X. F., van Loon, J. J., and Jansen, J. A. The effect of combined hypergravity and microgrooved surface topography on the behaviour of fibroblasts. *Cell Motil Cytoskeleton* 2006, 384-394, 2006.
  46. Teramoto, H., Coso, O. A., Miyata, H., Igishi, T., Miki, T., and Gutkind, J. S. Signaling from the small GTP-binding proteins Rac1 and Cdc42 to the c-Jun N-terminal kinase/stress-activated protein kinase pathway. A role for mixed lineage kinase 3/protein-tyrosine kinase 1, a novel member of the mixed lineage kinase family. *J Biol Chem* 1996, 27225-27228, 1996.
  47. Porras, A., Zuluaga, S., Black, E., Valladares, A., Alvarez, A. M., Ambrosino, C., Benito, M., and Nebreda, A. R. P38 alpha mitogen-activated protein kinase sensitizes cells to apoptosis induced by different stimuli. *Mol Biol Cell* 2004, 922-933, 2004.
  48. Secomb, T. W., Hsu, R., and Pries, A. R. Effect of the endothelial surface layer on transmission of fluid shear

stress to endothelial cells. *Biorheology* 2001, 143-150, 2001.